A consistent modelling methodology for secondary settling tanks: a reliable numerical method

Raimund Bürger, Stefan Diehl, Sebastian Farås, Ingmar Nopens and Elena Torfs

ABSTRACT

The consistent modelling methodology for secondary settling tanks (SSTs) leads to a partial differential equation (PDE) of nonlinear convection–diffusion type as a one-dimensional model for the solids concentration as a function of depth and time. This PDE includes a flux that depends discontinuously on spatial position modelling hindered settling and bulk flows, a singular source term describing the feed mechanism, a degenerating term accounting for sediment compressibility, and a dispersion term for turbulence. In addition, the solution itself is discontinuous. A consistent, reliable and robust numerical method that properly handles these difficulties is presented. Many constitutive relations for hindered settling, compression and dispersion can be used within the model, allowing the user to switch on and off effects of interest depending on the modelling goal as well as investigate the suitability of certain constitutive expressions. Simulations show the effect of the dispersion term on effluent suspended solids and total sludge mass in the SST. The focus is on correct implementation whereas calibration and validation are not pursued.

Key words | continuous sedimentation, partial differential equation, secondary clarifier, simulation model, wastewater treatment

Raimund Bürger
CI^{2}MA and Departamento de Ingeniería Matemática,
Facultad de Ciencias Físicas y Matemáticas,
Universidad de Concepción,
Casilla 160-C,
Concepción,
Chile

Stefan Diehl (corresponding author)
Sebastian Farås
Centre for Mathematical Sciences,
Lund University,
P.O. Box 118,
S-221 00 Lund,
Sweden
E-mail: *diehl@maths.lth.se*

Ingmar Nopens
Elena Torfs
BIOMATH,
Department of Mathematical Modelling,
Statistics and Bioinformatics,
Coupure Links 653,
B-9000 Gent,
Belgium

NOMENCLATURE

Numbers in round brackets refer to equation numbers

A	cross-sectional area of secondary settling tank (SST) [m^2]
B	depth of thickening zone [m]
C	concentration [kg/m^3]
$\hat{C}$	maximum point of f_{bk} [kg/m^3]
C_c	critical concentration [kg/m^3]
C_j	concentration in layer j (15) [kg/m^3]
C_{max}	maximum concentration [kg/m^3]
C_{min}	parameter in settling velocity function (11) [kg/m^3]
D	primitive of d_{comp} (16) [kg/(ms)]
$\tilde{D}$	approximate value of D [kg/(ms)]
F	(convective) flux function (5) [$kg/(m^2s)$]
G	Godunov numerical flux (20) [$kg/(m^2s)$]
H	height of clarification zone [m]
J_{comp}, J_{disp}	compressive and dispersive fluxes (17) and (18) [$kg/(m^2s)$]
M	parameter controlling discretization of C-axis (24) [–]
N	number of layers of SST [–]
Q	volumetric flow rate [m^3/s]
S	Stenstrom numerical flux (37) [$kg/(m^2s)$]
d_{comp}, d_{disp}	compression function (7) and dispersion function (9) [m^2/s]
f_{bk}	Kynch batch flux density function (6) [$kg/(m^2s)$]
g	acceleration of gravity [m/s^2]
i	index of concentrations along C-axis [–]
j	layer index [–]
n	time index [–]
r_h, r_p	parameters in settling velocity function (11) [m^3/kg]
r_V	parameter in Vesilind hindered settling function (10) [m^3/kg]
t	time [s]

doi: 10.2166/wst.2013.239

v_0 settling velocity of a single particle in unbounded fluid [m/s]
$\tilde{v}_0$ parameter in settling velocity function (11) [m/s]
v_{hs} hindered settling velocity [m/s]
z depth from feed level in SST [m]

Greek letters, subscripts and superscripts

ΔC stepsize of discretization of C-axis (24) [kg/m^3]
Δt time step of numerical method [s]
Δz layer width of numerical method [m]
Φ (total) flux (4) [kg/(m^{2}s)]
α parameter in effective solid stress function (12) [Pa]
α_1, α_2 parameters in dispersion coefficient (14) ([m^{-1}] and [s/m^2])
β parameter in effective solid stress function (12) [kg/m^3]
γ characteristic function (2), equals 1 inside and 0 outside SST
δ Dirac delta distribution [m^{-1}]
ρ_f, ρ_s densities of fluid and solids [kg/m^3]
σ_e effective solid stress [Pa]
e, f, u effluent, feed, underflow (subscripts)
num numerical (convective, compressive or dispersive) flux function (superscript)

INTRODUCTION

Scope

Bürger *et al.* (2011) advanced a consistent modelling methodology (CMM) for secondary settling tanks (SSTs) in wastewater treatment (WWT). The CMM is based on the conservation of mass, which can be cast into the following one-dimensional (1D) partial differential equation (PDE) of nonlinear convection–diffusion type for the solids concentration C as a function of depth z and time t:

$$\frac{\partial C}{\partial t}+\frac{\partial}{\partial z}F(C,z,t)=\frac{\partial}{\partial z}\left(\{\gamma(z)d_{\mathrm{comp}}(C)+d_{\mathrm{disp}}(z,Q_f(t))\}\frac{\partial C}{\partial z}\right)+\frac{Q_f(t)C_f(t)}{A}\delta(z). \quad (1)$$

The second term on the left-hand side models hindered settling combined with bulk flows. The expression in curled brackets models sediment compressibility and dispersion, and a singular source term models the feed mechanism. Equation (1) cannot be solved numerically by standard engineering textbook methods, since F is a discontinuous function of z, and d_{comp} vanishes over a range of concentration values.

Since the solution $C=C(z,t)$ of (1) may be discontinuous, this PDE does not hold in the classical pointwise sense. Instead, we must interpret it in the weak sense. This means that C only satisfies a particular integrated form of (1) which does not involve the partial derivatives $\partial C/\partial t$ and $\partial C/\partial z$, since such are ill-defined if C is discontinuous. Thus, numerical methods are usually derived from the conservation law integrated in space since one has to discretize the model, i.e. compute the concentration only at a finite number of layers of the SST and at discrete time points. A weak solution should also satisfy a so-called entropy condition, which singles out physically relevant discontinuities, i.e. that are stable with respect to small perturbations. Such a condition is standard for nonlinear conservation laws (see, for example, Le Veque (1992) and Anderson & Edwards (1981) for the context of sedimentation).

It is the purpose of this contribution to describe a consistent, reliable and robust numerical method for the simulation of 1D SSTs. The remaining steps of the CMM, i.e. calibration and validation, are not pursued here. Thus, the constitutive functions chosen for settling, compression and dispersion might not be the final ones since modifications might be required during the iterative model building process. The flexible CMM framework assists in this development.

A numerical method is *consistent* if the numerical flux (i.e. the flux of the numerical scheme) approximates the physical flux such that both coincide when discretization parameters tend to zero. A method is said to be *reliable* if the numerical solution is a good approximation of the exact solution of the model PDE. Thus, the numerical method should automatically take into account the entropy condition. Note that consistency alone does not ensure reliability. Furthermore, a numerical method is *robust* if it can handle all possible initial conditions and input dynamics, e.g. storm weather.

The most common simulation method in the WWT community is the one by Takács *et al.* (1991). For normal operating conditions, it behaves reasonably, but several shortcomings have been reported; see Jeppsson & Diehl (1996a, b), David *et al.* (2009a), Plósz *et al.* (2011), Bürger *et al.* (2011, 2012). The latter two references include simulations obtained by the method of Takács *et al.* (1991) that exhibit entropy-violating (physically unstable) discontinuities. We show here how existing implementations of the

simulation method of Takács *et al.* (1991) can be updated to become reliable.

The consistent, reliable and robust numerical method for the simulation of clarifier-thickener units by Bürger *et al.* (2005) was used for the simulation of SSTs by De Clercq *et al.* (2005, 2008). It utilizes the numerical flux by Engquist & Osher (1981). The numerical method presented here is based on the Godunov numerical flux (Godunov 1959). This method is slightly less accurate than the one by Bürger *et al.* (2005), but is easier to implement and requires fewer computations (Bürger *et al.* 2012). A method-of-lines formulation enables the simulation model to be used in conjunction with ODE (ordinary differential equation) solvers for the biokinetic model equations for the biological reactor.

Related works and novelty of this paper

Available SST simulators can roughly be divided into two categories. One contains the traditional layer models where certain rules control the flux between neighbouring layers and/or additional heuristic assumptions have been included directly into the numerical method (Stenstrom 1976; Attir & Denn 1978; Vitasovic 1989; Takács *et al.* 1991; Dupont & Henze 1992; Otterpohl & Freund 1992; Härtel & Pöpel 1992; Koehne *et al.* 1995; Watts *et al.* 1996; Chatellier & Audic 2000; Queinnec & Dochain 2001; Giokas *et al.* 2002; Verdickt *et al.* 2005; Plósz *et al.* 2007, 2011; Abusam & Keesman 2009; David *et al.* 2009a, b). Such heuristic rules and assumptions normally imply unreliable simulators (Bürger *et al.* 2012). In the other category, the simulator is derived from the governing PDE (Anderson & Edwards 1981; Lev *et al.* 1986; Chancelier *et al.* 1997; Diehl & Jeppsson 1998; Mazzolani *et al.* 1998; Wett 2002; De Clercq *et al.* 2003; Griborio 2004; McCorquodale *et al.* 2004; Martin 2004; Bürger *et al.* 2005). It is, however, difficult to assess whether a particular numerical implementation is reliable even if it is rigorously derived from the governing PDE. Of all these publications, only Bürger *et al.* (2005) have presented a proved reliable numerical method, which can be used to evaluate other simulators.

The main novelty of this paper is a new SST simulator which is easier to implement than the reference method but still yields very similar simulation results (Bürger *et al.* 2012), from which we conjecture that it is reliable. Moreover, most effects found in previous 1D SST simulators (hindered settling, dispersion, compression) can be turned on or off to the user's convenience, which makes it flexible and powerful. The limitations of models restricted to 1D have been discussed by Ekama *et al.* (1997). They conclude that one way to capture different 3D phenomena, which have a smoothing effect on concentration gradients, is the inclusion of a 'pseudo-diffusivity coefficient' at the place of the expression in curled brackets in (1). The model (1) can thus be seen as an extension of the pseudo-diffusivity coefficient. Moreover, in (1) compression and dispersion are modelled by separate terms, which should allow the use of measured data (e.g. settling velocity parameters) as such in the model.

Outline of the paper

The next section explains the mathematical model with its constitutive assumptions. Then, in a longer section, the discretization of the model and the implementation are described. We present partly a method-of-lines formulation, which consists of one ODE for each layer, and partly a fully discrete numerical method in which the unavoidable time-step restriction (Courant–Friedrichs–Lewy (CFL) condition) is given. Of particular interest is the relation of the Godunov numerical flux with the method of Takács *et al.* (1991). In another section we demonstrate how to convert an existing implementation of Takács' simulation method into the present method. A section on simulations follows, and then a discussion and conclusions end the paper.

MATHEMATICAL MODEL

Idealizing assumptions and the conservation law

The volumetric flows leaving the idealized SST (Figure 1) at the underflow and effluent levels ($z = B$ and $z = -H$, respectively) are denoted by Q_u and Q_e, respectively, where $Q_u, Q_e \geq 0$. We assume that there is either an upward (Q_e) or a downward (Q_u) volumetric flow at each point of the downward-pointing z-axis, except for $z = 0$, where the feed source is located. Horizontal currents, wall effects, raking, and other features are neglected. Moreover, we assume that the SST is cylindrical with a constant cross-sectional area A.

The z-axis can be divided into the effluent zone ($z < -H$), the clarification zone ($-H < z < 0$), the thickening zone ($0 < z < B$), and the underflow zone ($z > B$). The following function indicates whether z is a coordinate in the interior or the exterior of the SST:

$$\gamma(z) := \begin{cases} 1 & \text{for } -H \leq z \leq B, \\ 0 & \text{for } z < -H \text{ or } z > B. \end{cases} \quad (2)$$

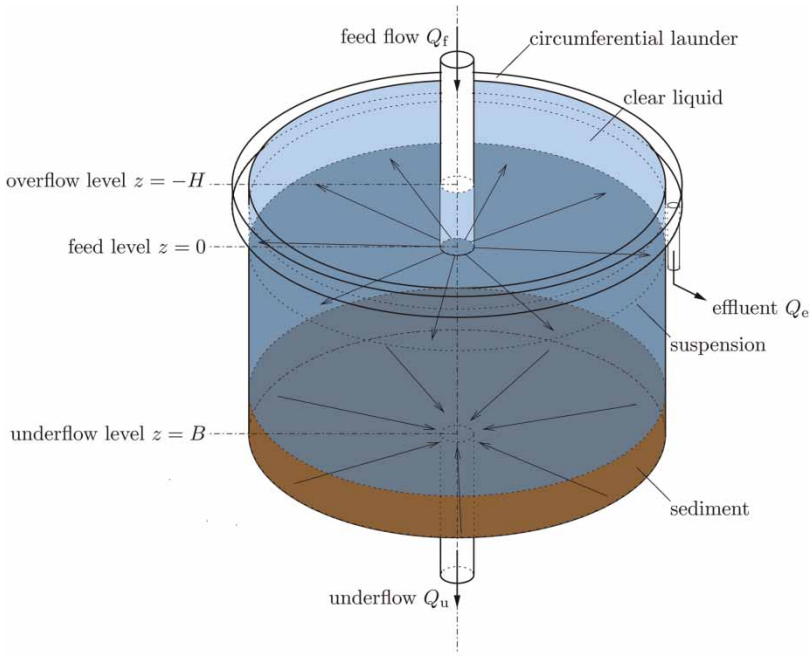

Figure 1 | Schematic illustration of the SST. The height of the clarification zone is denoted by H and the depth of the thickening zone by B.

The conservation law of mass states that the rate of increase of mass in an arbitrary interval (z_1, z_2) of the depth axis equals the flux in $(\Phi|_{z=z_1})$ minus the flux out $(\Phi|_{z=z_2})$ plus the production inside the interval:

$$\frac{\mathrm{d}}{\mathrm{d}t}\int_{z_1}^{z_2} AC(z,t)\,\mathrm{d}z = A\left(\Phi|_{z=z_1} - \Phi|_{z=z_2}\right) + \int_{z_1}^{z_2} Q_f(t)C_f(t)\delta(z)\,\mathrm{d}z, \tag{3}$$

where $Q_f = Q_e + Q_u$ is the volumetric feed flow, C_f is the feed concentration and

$$\Phi\left(C, \frac{\partial C}{\partial z}, z, t\right) = F(C,z,t) - (\gamma(z)d_{comp}(C) + d_{disp}(z, Q_f(t)))\frac{\partial C}{\partial z} \tag{4}$$

is the total flux. Here,

$$F(C,z,t) := \begin{cases} -Q_e(t)C/A & \text{for } z < -H, \\ -Q_e(t)C/A + f_{bk}(C) & \text{for } -H \le z < 0, \\ Q_u(t)C/A + f_{bk}(C) & \text{for } 0 < z \le B, \\ Q_u(t)C/A & \text{for } z > B \end{cases} \tag{5}$$

is the convective flux function, which involves the Kynch batch flux density function

$$f_{bk}(C) := Cv_{hs}(C), \tag{6}$$

where $v_{hs}(C)$ is the hindered settling velocity (Kynch 1952). The function $d_{comp} = d_{comp}(C)$ accounts for sediment compressibility, and the dispersion function $d_{disp} = d_{disp}(z, Q_f)$ incorporates mixing of lower and higher sludge concentrations by 'lumping' together several mechanisms related to density and turbulent currents.

Equation (3) is the model in integral form. Note that Equations (3)–(5) do not contain the cross-sectional areas of the outlet pipes. We are interested only in the concentrations in the outlet pipes and not the bulk velocities. Under the assumption that the particles follow the water streams in the outlet pipes, the outlet concentrations are independent of the areas of the pipes (Diehl 2000).

The compression function d_{comp} is given by Bürger *et al.* (2005)

$$d_{comp}(C) = \frac{\rho_s}{(\rho_s - \rho_f)g} v_{hs}(C)\sigma_e'(C), \tag{7}$$

where ρ_s and $\rho_f < \rho_s$ are the (constant) solid and fluid mass densities, g is the acceleration of gravity, and

$\sigma_e = \sigma_e(C)$ is the effective solid stress function, whose derivative satisfies

$$\sigma_e'(C)\begin{cases} = 0 & \text{for } 0 \le C < C_c, \\ > 0 & \text{for } C > C_c, \end{cases} \tag{8}$$

where C_c is a material-dependent critical concentration which the solid particles start to touch each other.

The dispersion function d_{disp} is often set as the product of the fluid velocity and some characteristic length scale (Anderson & Edwards 1981; Lee *et al.* 2006). To capture mixing phenomena caused by the feed inlet, we set

$$d_{disp}(z, Q_f(t)) = \frac{Q_f(t)}{A} L(z, Q_f(t)),$$

where L is a continuous function, which is zero some distance away from the inlet. The model captures that once a portion of suspended sludge has left the SST through one of the outlets it cannot return, if we restrict dispersion to the interior of the tank by setting

$$d_{disp}(z, Q_f(t))\begin{cases} = 0 & \text{for } z \le -H \text{ and } z \ge B, \\ \ge 0 & \text{for } -H < z < B. \end{cases} \tag{9}$$

The ingredients d_{comp} and d_{disp} are independent from each other, and we may set $d_{comp} \equiv 0$ or $d_{disp} \equiv 0$ for materials and SSTs that do not exhibit sludge compressibility or dispersion. This provides high flexibility in model use. In the presented numerical method, both options are explicitly included and not lumped as in others. Therefore one can explicitly distinguish between phenomena in the model, which will be advantageous in the calibration and validation phase of the model building process (outside the scope of this paper).

Given initial data at $t = 0$, we call the (entropy-satisfying) solution of Equation (1), interpreted in the weak sense, the *exact* solution of the model. A numerical solution is always an approximation of the exact solution. Equation (1) can be solved without imposing boundary conditions on C. Only initial data $C(z, 0)$ must be given. All boundary concentrations are outputs of the model and should not be prescribed.

Constitutive functions

Note that no model parameters have appeared so far. According to CMM such parameters are introduced only in the constitutive functions, which in our model are $v_{hs}(C)$, $\sigma_e(C)$ and $d_{disp}(z, Q_f)$. One of the strengths of the model above and the numerical method presented below is that any (reasonable) constitutive functions with model parameters can be included. It is not our intention to promote any of the used constitutive functions. Thorough calibration/validation based on dedicated experimental data should in the future indicate which constitutive functions (those presented here or elsewhere in the literature) can better describe the real SST behaviour.

For the hindered settling velocity, one common choice is

$$v_{hs}(C) = v_0 e^{-r_V C}, \tag{10}$$

where v_0 is the maximum theoretical settling velocity and $r_V > 0$ is a parameter (Vesilind 1968). Another popular expression is the double exponential function by Takács *et al.* (1991) (rewritten by Diehl & Jeppsson (1998) so that $v_{hs}(C) \ge 0$):

$$v_{hs}(C) = \max\{0, \min\{\tilde{v}_0, v_0(e^{-r_h(C-C_{min})} - e^{-r_p(C-C_{min})})\}\}, \tag{11}$$

where $\tilde{v}_0$ and v_0 are the maximal practical and theoretical settling velocities, respectively, r_h and r_p are settling parameters, and C_{min} is the concentration below which $v_{hs} = 0$. More involved settling velocity functions $v_{hs}(C)$ have been proposed that intend to handle discrete settling at low concentrations. However, they are not yet mainstream, nor extensively calibrated/validated and not tested here, though this could easily be done by the CMM.

For the effective solid stress $\sigma_e(C)$, De Clercq *et al.* (2008) propose the following semi-empirical formula based on inverse modelling using experimental data:

$$\sigma_e(C) = \begin{cases} 0 & \text{for } C < C_c, \\ \alpha \ln\left(1 + \dfrac{C - C_c}{\beta}\right) & \text{for } C \ge C_c \end{cases} \tag{12}$$

with empirical parameters $\alpha, \beta > 0$. Empirical constitutive functions have been suggested for d_{comp} directly (Vaccari & Uchrin 1989; Cacossa & Vaccari 1994). We prefer the physically motivated formula (7), which involves both constitutive relations v_{hs} and σ_e. In our simulations we use (10) and (12), which together with the property (8) means that

$$d_{comp}(C) = \begin{cases} 0 & \text{for } 0 \le C < C_c, \\ \dfrac{\rho_s \alpha v_0 e^{-r_V C}}{g(\rho_s - \rho_f)(\beta + C - C_c)} & \text{for } C \ge C_c. \end{cases} \tag{13}$$

As for the dispersion function d_{disp}, one may use any continuous function satisfying (9). For our simulations, we

have chosen

$$d_{\mathrm{disp}}(z, Q_{\mathrm{f}}) = \begin{cases} \alpha_1 Q_{\mathrm{f}} \exp\left(\dfrac{-z^2/(\alpha_2 Q_{\mathrm{f}})^2}{1-|z|/(\alpha_2 Q_{\mathrm{f}})}\right) & \text{for } |z|<\alpha_2 Q_{\mathrm{f}}, \\ 0 & \text{for } |z| \geq \alpha_2 Q_{\mathrm{f}}. \end{cases} \tag{14}$$

where α_1 and α_2 are positive parameters (and α_1 contains A). In particular, $\alpha_2 Q_{\mathrm{f}}$ determines the width of the dispersion region. In view of (9), we require that

$$\alpha_2 < \frac{\min(H, B)}{\max_{t\geq 0} Q_{\mathrm{f}}(t)}.$$

DISCRETIZATION OF THE MATHEMATICAL MODEL

Subdivision into layers

We subdivide the tank into N internal layers, so that each layer has the depth $\Delta z = (B+H)/N$. The boundaries between the layers are located at positions $z_j := j\Delta z - H$ for $j = 0, \ldots, N$ (see Figure 2). Thus, $z_0 = -H$ and $z_N = B$. We will refer to 'layer j' as the interval $[z_{j-1}, z_j]$. In view of the left-hand side of (3), we define $C_j = C_j(t)$ as the average of the exact solution C over layer j at time t (see Figure 2):

$$C_j(t) := \frac{1}{\Delta z} \int_{z_{j-1}}^{z_j} C(z, t)\, \mathrm{d}z. \tag{15}$$

Define $j_{\mathrm{f}} := \lceil H/\Delta z \rceil$ to be the smallest integer larger or equal to $H/\Delta z$. Then the feed inlet ($z = 0$) is located in the 'feed layer' $(z_{j_{\mathrm{f}}-1}, z_{j_{\mathrm{f}}})$. Two layers are added to both the top and bottom corresponding to the effluent and underflow zones, respectively (in principle, one could add more layers in these zones to model the concentration propagation in the outlet pipes). These four layers are necessary for a correct numerical implementation for two reasons: for the approximation of spatial derivatives and for the computation of the outlet concentrations. Thus, the computational domain is composed of $N+4$ intervals of length Δz, enclosed by the points z_j, $j = -2, \ldots, N+2$. This ingredient differs from most published SST simulators, which erroneously assume that the concentration is always continuous across the outlet locations, i.e. the outlet concentrations are the same as in layer 1 and N, respectively. Bürger *et al.* (2012) explain why this is erroneous. In the present method, the effluent (underflow) concentration C_{e} (C_{u}) is instead found in the effluent- (underflow-) zone layers:

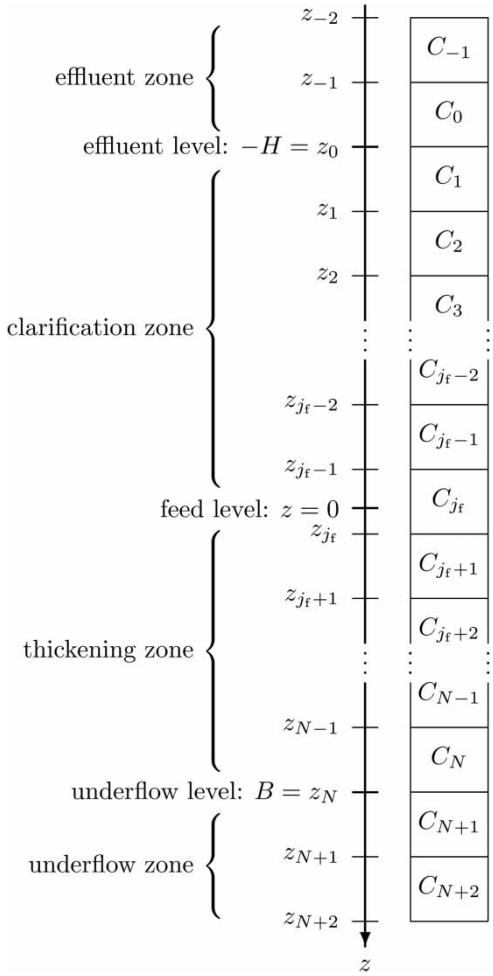

Figure 2 | Schematic illustration of the subdivision of the computational domain into layers. The height of the clarification zone is denoted by H, and the depth of the thickening zone by B.

$$C_{\mathrm{e}}(t) := C_{-1}(t) \quad \text{and} \quad C_{\mathrm{u}}(t) := C_{N+2}.$$

The conservation law for each layer

The numerical method is derived by first rewriting the governing Equation (3) in a slightly different form. We define the primitive of d_{comp},

$$D(C) := \int_{C_{\mathrm{c}}}^{C} d_{\mathrm{comp}}(s)\, \mathrm{d}s, \tag{16}$$

so that

$$d_{\mathrm{comp}}(C)\frac{\partial C}{\partial z}=\frac{\partial}{\partial z}D(C).$$

We can then write (4) as $\Phi = F - J_{\mathrm{disp}} - J_{\mathrm{comp}}$, where

$$J_{\mathrm{disp}}(z,t) := d_{\mathrm{disp}}(z, Q_{\mathrm{f}}(t))\frac{\partial C}{\partial z}, \tag{17}$$

$$J_{\mathrm{comp}}(z,t) := \gamma(z)\frac{\partial D(C)}{\partial z}. \tag{18}$$

Equation (3) can now be rewritten, for each layer j, by dividing by A and Δz, as follows:

$$\begin{aligned}\frac{\mathrm{d}C_j}{\mathrm{d}t} = &-\frac{F(C(z_j,t),z_j,t)-F(C(z_{j-1},t),z_{j-1},t)}{\Delta z}\\ &+\frac{J_{\mathrm{disp}}(z_j,t)-J_{\mathrm{disp}}(z_{j-1},t)}{\Delta z}+\frac{J_{\mathrm{comp}}(z_j,t)-J_{\mathrm{comp}}(z_{j-1},t)}{\Delta z}\\ &+\frac{1}{\Delta z}\int_{z_{j-1}}^{z_j}\frac{Q_{\mathrm{f}}(t)C_{\mathrm{f}}(t)}{A}\delta(z)\mathrm{d}z.\end{aligned} \tag{19}$$

The finite difference quotients of F, J_{disp} and J_{comp} are not approximations of derivatives; they follow from the conservation law for a layer.

Approximation of the convective flux

The convective flux $F(C(z_j,t),z_j,t)$ in (19) at the boundary between layers j and $j+1$ should be replaced by a numerical convective flux F_j^{num} associated with position z_j. Such a numerical flux will in general depend on the adjacent layer concentrations $C_j(t)$ and $C_{j+1}(t)$, i.e.

$$F_j^{\mathrm{num}}(C_j(t),C_{j+1}(t),t)\approx F(C(z_j,t),z_j,t).$$

There are several reasonable choices of F_j^{num}, and restrictions that must be met to ensure convergence to the exact solution; see Bürger *et al.* (2012).

Since a simulator of the SST should eventually be included in a model of an entire WWT plant, the simulation speed is important. Therefore, we choose here the Godunov numerical flux (Godunov 1959) on f_{bk} as an approximation of $f_{\mathrm{bk}}(C(z_j,t))$:

$$G_j = G_j(C_j,C_{j+1}) = \begin{cases}\min\limits_{C_j\le C\le C_{j+1}} f_{\mathrm{bk}}(C) & \text{if } C_j\le C_{j+1},\\ \max\limits_{C_j\ge C\ge C_{j+1}} f_{\mathrm{bk}}(C) & \text{if } C_j > C_{j+1}.\end{cases} \tag{20}$$

The computation of G_j is greatly simplified whenever f_{bk} has precisely one local maximum at $C=\hat{C}$ (e.g. for (10), we have $\hat{C}=1/r_{\mathrm{V}}$). Evaluating (20) with all possible orderings of C_j, C_{j+1} and $\hat{C}$ shows that G_j can then be computed by the following simple algorithm.

Algorithm 1 (Computation of G_j)
Input: concentrations C_j and C_{j+1}, function f_{bk} with exactly one maximum at $\hat{C}$
Output: value of G_j
if $C_j \le C_{j+1}$ **then**
  $G_j \leftarrow \min\{f_{\mathrm{bk}}(C_j), f_{\mathrm{bk}}(C_{j+1})\}$
else
  if $(\hat{C}-C_j)\cdot(\hat{C}-C_{j+1})<0$ **then**
    $G_j \leftarrow f_{\mathrm{bk}}(\hat{C})$
  else
    $G_j \leftarrow \max\{f_{\mathrm{bk}}(C_j), f_{\mathrm{bk}}(C_{j+1})\}$
  endif
endif

Summarizing, we obtain the numerical flux

$$\begin{aligned}F_j^{\mathrm{num}} &= F_j^{\mathrm{num}}(C_j,C_{j+1},t)\\ &:= \begin{cases}-(Q_{\mathrm{e}}(t)/A)C_{j+1} & \text{for } j=-2,\ -1,\\ -(Q_{\mathrm{e}}(t)/A)C_{j+1}+G_j & \text{for } j=0,\ \ldots,\ j_{\mathrm{f}}-1,\\ (Q_{\mathrm{u}}(t)/A)C_j+G_j & \text{for } j=j_{\mathrm{f}},\ \ldots,\ N,\\ (Q_{\mathrm{u}}(t)/A)C_j & \text{for } j=N+1,\ N+2,\end{cases}\end{aligned} \tag{21}$$

where G_j is given by (20) or Algorithm 1.

Approximation of the dispersion and compression fluxes

We approximate (17) by

$$J_{\mathrm{disp}}(z_j,t)\approx J_{\mathrm{disp},j}^{\mathrm{num}} := d_{\mathrm{disp},j}\frac{C_{j+1}-C_j}{\Delta z}, \tag{22}$$

where we set $d_{\mathrm{disp},j} := d_{\mathrm{disp}}(z_j, Q_{\mathrm{f}}(t))$. Analogously, we approximate (18) as

$$J_{\mathrm{comp}}(z_j,t)\approx J_{\mathrm{comp},j}^{\mathrm{num}} := \gamma(z_j)\frac{D_{j+1}^{\mathrm{num}}-D_j^{\mathrm{num}}}{\Delta z}, \tag{23}$$

where D_j^{num} is either the exact or an approximate integrated compression coefficient (16). For some choices of v_{hs} and σ_e, the primitive D of d_{comp} can be expressed in closed form (see, for example, Bürger & Karlsen 2001). Then we can simply define $D_j^{\text{num}} := D(C_j)$ (exact primitive). If an exact primitive cannot be found, we approximate $D(C_j)$ by numerical integration. To obtain fast simulations, one can avoid evaluating the integral in (16) at every time step. This technique involves two steps. Before the simulation starts, use the trapezoidal rule to compute approximate values $\tilde{D}_i$ of $D(i\Delta C)$ on a finely discretized C–axis at

$$C_c + i\Delta C, \quad i = 0, 1, \ldots, M, \tag{24}$$

where $M\Delta C = C_{\max} - C_c$ should hold, and $C_{\max}$ is a chosen maximum concentration. During the simulation, we determine the approximate value D_j^{num} of $D(C_j)$ by linear interpolation. This two-step procedure introduces an error, which depends on ΔC or, equivalently, M. Without going into details, one should choose ΔC proportional to $(\Delta z)^{3/2}$ (M proportional to $N^{3/2}$) in order not to destroy the overall order of convergence when the approximation (23) is made. Since precomputations do not influence the running simulation time, we reduce the error further by setting $M = N^2$. Furthermore, if $d_{\text{comp}}(C)$ is discontinuous at $C = C_c$, make sure that $d_{\text{comp}}(C_c) > 0$ in Algorithm 2, cf. (13).

Algorithm 2 (Precomputation of $\tilde{D}_i$)
Inputs: number of layers N, critical concentration C_c, maximum concentration $C_{\max}$, function d_{comp}
Outputs: value ΔC, values $\tilde{D}_i$, $i = 0, 1, \ldots, M$
$M \leftarrow N^2$
$\Delta C \leftarrow (C_{\max} - C_c)/M$
$\tilde{D}_0 \leftarrow 0$
$d_0 \leftarrow d_{\text{comp}}(C_c)$
for $i = 1, \ldots, M$
  $d_i \leftarrow d_{\text{comp}}(C_c + i\Delta C)$
  $\tilde{D}_i \leftarrow \tilde{D}_{i-1} + \frac{\Delta C}{2}(d_{i-1} + d_i)$
endfor

During the simulation, given a layer concentration $C_j > C_c$, we use linear interpolation between $\tilde{D}_i$ and $\tilde{D}_{i+1}$ for a suitable index i to define D_j^{num}. This index i thus satisfies $C_c + i\Delta C \le C_j < C_c + (i+1)\Delta C$. The algorithm is the following, where $\lfloor x \rfloor$ is the nearest integer below the real number x.

Algorithm 3 (Computation of D_j^{num})
Inputs: values j, ΔC, C_j and $\tilde{D}_i$, $i = 0, 1, \ldots, M$
Output: value D_j^{num}
if $C_j \le C_c$
  $D_j^{\text{num}} \leftarrow 0$
else
  $i \leftarrow \left\lfloor \frac{(C_j - C_c)}{\Delta C} \right\rfloor$
  $D_j^{\text{num}} \leftarrow \tilde{D}_i + \left(\tilde{D}_{i+1} - \tilde{D}_i\right)\left(\frac{C_j - C_c}{\Delta C} - i\right)$
endif

Method of lines

Substituting the numerical fluxes into the exact version of the conservation law (19) yields the approximate method-of-lines formula

$$\frac{dC_j}{dt} = -\frac{F_j^{\text{num}} - F_{j-1}^{\text{num}}}{\Delta z} + \frac{1}{\Delta z}\left(J_{\text{disp},j}^{\text{num}} - J_{\text{disp},j-1}^{\text{num}} + J_{\text{comp},j}^{\text{num}} - J_{\text{comp},j-1}^{\text{num}}\right) + \frac{Q_f C_f}{A\Delta z}\delta_{j,j_f}, \quad j = -1, \ldots, N+2, \tag{25}$$

where $\delta_{j,j_f} = 1$ if $j = j_f$ and $\delta_{j,j_f} = 0$ otherwise. (Recall that $j = -1$ and $j = 0$ correspond to the layers of the effluent zone, $[z_{-2}, z_{-1}]$ and $[z_{-1}, z_0]$.) The expressions F_j^{num}, $J_{\text{disp},j}^{\text{num}}$ and $J_{\text{comp},j}^{\text{num}}$ are defined by (21), (22) and (23), respectively. Formula (25) is an approximation of the exact conservation law formulation (19).

Not all of the terms in (25) are present in every layer. Explicitly, we obtain for the layers with $j = -1$ and $j = 0$ located in the effluent zone:

$$\frac{dC_{-1}}{dt} = \frac{Q_e}{A\Delta z}(C_0 - C_{-1}), \tag{26}$$

$$\frac{dC_0}{dt} = \frac{Q_e}{A\Delta z}(C_1 - C_0) - \frac{G_0}{\Delta z} + \frac{D_1^{\text{num}} - D_0^{\text{num}}}{(\Delta z)^2}, \tag{27}$$

for layer 1 within the SST:

$$\frac{dC_1}{dt} = \frac{Q_e}{A\Delta z}(C_2 - C_1) - \frac{G_1 - G_0}{\Delta z} + \frac{d_{\text{disp},1}(C_2 - C_1) + D_2^{\text{num}} - 2D_1^{\text{num}} + D_0^{\text{num}}}{(\Delta z)^2}, \tag{28}$$

for layers $j = 2, \ldots, j_f - 1$:

$$\frac{dC_j}{dt} = \frac{Q_e}{A\Delta z}(C_{j+1} - C_j) - \frac{G_j - G_{j-1}}{\Delta z} + \frac{d_{disp,j}(C_{j+1} - C_j) - d_{disp,j-1}(C_j - C_{j-1})}{(\Delta z)^2} + \frac{D_{j+1}^{num} - 2D_j^{num} + D_{j-1}^{num}}{(\Delta z)^2}, \quad (29)$$

for the feed layer $j = j_f$:

$$\frac{dC_{j_f}}{dt} = -\frac{Q_u + Q_e}{A\Delta z}C_{j_f} - \frac{G_{j_f} - G_{j_f-1}}{\Delta z} + \frac{d_{disp,j_f}(C_{j_f+1} - C_{j_f}) - d_{disp,j_f-1}(C_{j_f} - C_{j_f-1})}{(\Delta z)^2} + \frac{D_{j_f+1}^{num} - 2D_{j_f}^{num} + D_{j_f-1}^{num}}{(\Delta z)^2} + \frac{Q_f C_f}{A\Delta z}, \quad (30)$$

for the layers with $j = j_f + 1, \ldots, N - 1$ in the thickening zone:

$$\frac{dC_j}{dt} = -\frac{Q_u}{A\Delta z}(C_j - C_{j-1}) - \frac{G_j - G_{j-1}}{\Delta z} + \frac{d_{disp,j}(C_{j+1} - C_j) - d_{disp,j-1}(C_j - C_{j-1})}{(\Delta z)^2} + \frac{D_{j+1}^{num} - 2D_j^{num} + D_{j-1}^{num}}{(\Delta z)^2}, \quad (31)$$

for the bottom layer in the thickening zone:

$$\frac{dC_N}{dt} = -\frac{Q_u}{A\Delta z}(C_N - C_{N-1}) - \frac{G_N - G_{N-1}}{\Delta z} + \frac{-d_{disp,N-1}(C_N - C_{N-1}) + D_{N+1}^{num} - 2D_N^{num} + D_{N-1}^{num}}{(\Delta z)^2}, \quad (32)$$

for the two layers that form the underflow zone:

$$\frac{dC_{N+1}}{dt} = -\frac{Q_u}{A\Delta z}(C_{N+1} - C_N) + \frac{G_N}{\Delta z} - \frac{D_{N+1}^{num} - D_N^{num}}{(\Delta z)^2}, \quad (33)$$

$$\frac{dC_{N+2}}{dt} = -\frac{Q_u}{A\Delta z}(C_{N+2} - C_{N+1}). \quad (34)$$

Time discretization

The method of lines (26)–(34) can be implemented when ODE solvers are available. This is particularly handy when the SST should be simulated together with other ODEs modelling the biological reactions of an activated sludge process (ASP). However, since the spatial accuracy of the scheme is only of first order, there is probably not much to gain in terms of speed by using any high-order-in-time ODE solver. A simple explicit Eulerian time step is sufficient. To this end, we select a time step $\Delta t > 0$ according to the CFL condition, see (36), and let $t_n := n\Delta t$, $n = 0, 1, 2, \ldots$. We denote by C_j^n the value of the layer concentration at time t_n, cf. (15),

$$C_j^n := C_j(t_n) = \frac{1}{\Delta z}\int_{z_{j-1}}^{z_j} C(z, t_n)\,dz, \qquad j = -1, \ldots, N + 2.$$

We approximate the time derivative in (26)–(34) by the explicit Euler step

$$\frac{dC_j}{dt}(t_n) \approx \frac{C_j^{n+1} - C_j^n}{\Delta t},$$

evaluate the right-hand side of (25) at $t = t_n$, and replace $C_j(t_n)$ by C_j^n. Multiplying the resulting equation by Δt and adding C_j^n to both sides we obtain the fully discrete method

$$C_j^{n+1} = C_j^n - \frac{\Delta t}{\Delta z}(F_j^{num,n} - F_{j-1}^{num,n}) + \frac{\Delta t}{\Delta z}(J_{disp,j}^{num,n} - J_{disp,j-1}^{num,n} + J_{comp,j}^{num,n} - J_{comp,j-1}^{num,n}) + \frac{\Delta t}{\Delta z}\frac{Q_f(t_n)C_f(t_n)}{A}\delta_{j,j_f}, \quad j = -1, \ldots, N + 2, \quad (35)$$

where $F_j^{num,n} := F_j^{num}(C_j, C_{j+1}, t_n)$, etc. We omit writing out (35) for each layer.

CFL condition

Suppose we want to use (35) to simulate an SST over a time interval $[0, T]$. Given a layer depth Δz, we must choose the time step Δt such that the condition

$$\Delta t \le \left[\frac{1}{\Delta z}\left(\max_{0\le t\le T}\frac{Q_f(t)}{A} + \max_{0\le C\le C_{max}}|f'_{bk}(C)|\right) + \frac{2}{(\Delta z)^2}\left(\max_{0\le C\le C_{max}} d_{comp}(C) + \max_{-H\le z\le B, 0\le t\le T} d_{disp}(z, Q_f(t))\right)\right]^{-1} \quad (36)$$

is satisfied. Inequality (36) yields an upper limit of the time step Δt. Such a limit must be submitted into any ODE solver for the method of lines (25). A condition like (36) is known in numerical analysis as a 'CFL condition'. It is necessary to

ensure stability of the numerical scheme. One should choose $C_{\max}$ sufficiently large (above C_c), where f_{bk} and its derivative are almost zero. Then $d_{comp}(C)$ is also small. Whether $C_{\max}$ is set to, for example, 20 or 30 kg/m^3 has no impact on the simulation time.

HOW TO CONVERT THE METHOD BY TAKÁCS *ET AL.* (1991) TO A RELIABLE ONE

The simulation method by Takács *et al.* (1991) is implemented in many SST simulators. It can be converted to a reliable method with the following steps.

Upgrade the numerical flux

The method by Takács *et al.* (1991) is roughly the one by Vitasovic (1989) with the specific constitutive relation given by (11). The key ingredient is, however, the numerical flux update due to Stenstrom (1976):

$$S_j = \min\{f_{bk}(C_j), f_{bk}(C_{j+1})\}. \quad (37)$$

The Stenstrom–Vitasovic–Takács (SVT) flux S_j in (37) should be compared with the Godunov flux G_j in (20), which contains a minimum function, however over an entire interval instead of only at the two concentration values C_j and C_{j+1}. When f_{bk} has precisely one maximum (the only realistic case), G_j can be computed by Algorithm 1, where (37) can be found in the first if–then statement. Hence, the SVT flux (37) can easily be upgraded to the reliable Godunov flux by adding a few lines in the simulation program.

A fundamental CMM principle is that all model parameters should be included in the physical constitutive assumptions only, so that they appear in the model PDE and then are carried over to any numerical method. No parameters should be introduced in the numerical algorithm itself. Consequently, the threshold suspended solids concentration X_t in the clarification zone layers in the method by Takács *et al.* (1991) should be removed.

Upgrade the outlet concentrations

The Takács method assumes that the concentration in the top layer inside the SST is the same as in the effluent. In some situations, this is a non-physical assumption which the present simulation method avoids. The physically correct approach consists of enforcing the conservation of mass also across the outlets, i.e. the flux of particles leaving the top layer should be equal to what the effluent pipe receives. The effluent concentration is a part of the solution of the model Equation (1), namely in $z < -H$. (The analogous situation holds at the bottom of the SST.) Recall that the assumption is that there is only bulk transport (neither settling, nor compression nor dispersion) outside the SST. In the numerical method, correct outlet concentrations are automatically obtained by means of the extra layers outside the SST.

Add compression and dispersion effects

To be able to calculate approximations of the second-order spatial derivative effects, one must add two extra layers at the top and bottom, respectively, outside the SST. The dispersion flux (22) is straightforwardly included when a constitutive relation for $d_{disp}(z, Q_f)$ has been chosen.

The numerical implementation of the compression flux needs some more care, since there are pitfalls; see Section 4.6 of Bürger *et al.* (2012) for an example where a natural straightforward discretization of the compression term yields incorrect numerical solutions, where the incorrectness becomes visible in a wrong simulated sludge blanket height. Once a constitutive function for d_{comp} has been chosen, it is important to first find the primitive of this, which often has to be done numerically with the precomputation in Algorithm 2.

Add the CFL condition

Defining the time step Δt such that the CFL condition (36) is satisfied, the method-of-lines formulas (26)–(34) or the fully discrete method (35) can be used to obtain stable, physically relevant solutions. Otherwise, non-physical solutions may appear, e.g. having small oscillations or negative concentrations.

SIMULATIONS

The possibilities of turning on and off optional compression and dispersion effects with the proposed method have been demonstrated by Bürger *et al.* (2011). Here, we investigate further the effect of dispersion on the outlet concentrations and on the transitions between different steady states. Most challenges to numerical methods for the model PDE (1) occur at the feed level and at the sludge blanket level.

We therefore simulate a scenario with a highly loaded SST and a sludge blanket close to the feed level. This can be accomplished in different ways. We have chosen a lower value of v_0 to simulate a sludge with bad settling properties caused by, for example, a salt shock which happens in winter or a toxic event. We use the same constitutive functions v_{hs}, σ_{e} and d_{disp} as in Bürger *et al.* (2012), namely (10), (12) and (14). Thus, compression is always present and d_{comp} is given by (13). For the constants in those functions, we set $v_0 = 3.47$ m/h, $r_{\mathrm{V}} = 0.37$ m^3/kg, $\alpha = 4.00$ Pa, $\beta = 4.00$ kg/m^3, $\rho_{\mathrm{s}} = 1,050$ kg/m^3, $\Delta\rho = 52$ kg/m^3, $g = 9.81$ m/s^2 and $C_{\mathrm{c}} = 6.00$ kg/m^3. These values are the same as in Bürger *et al.* (2011, 2012), so results can be compared. The nature of the SST response does not depend so much on the choice of parameters in v_{hs} and σ_{e} but on that of the functional forms, which coincide with those of De Clercq *et al.* (2008). In particular, the chosen form of σ_{e} (12) places maximal compressibility at the critical concentration C_{c}. Calibration of these parameters with experimental data was beyond the scope of this paper. The intent is to show what phenomena can be simulated with the model.

The constants α_1 and α_2 in (14) will be varied to illustrate their respective effect. In (36) we choose $C_{\max} = 20$ kg/m^3. We consider an SST with $H = 1$ m, $B = 3$ m and $A = 400$ m^2, and let the number of internal layers (within the SST) be $N = 90$ (i.e. a total of 94 layers for the numerical method).

In the first three simulations, the volumetric flows are kept constant: $Q_{\mathrm{f}} = 250$ m^3/h, $Q_{\mathrm{u}} = 80$ m^3/h; hence $Q_{\mathrm{e}} = 170$ m^3/h for $0 \le t \le 800$ h. The feed concentration is chosen as

$$C_{\mathrm{f}}(t) = \begin{cases} 4.0 \text{ kg/m}^3, & 0 \le t < 50 \text{ h}, \\ 3.7 \text{ kg/m}^3, & 50 \le t < 250 \text{ h}, \\ 4.1 \text{ kg/m}^3, & 250 \le t < 800 \text{ h}. \end{cases}$$

The SST is initially in a steady state with a sludge blanket level at the depth 0.6 m obtained from a simulation without dispersion, i.e. $\alpha_1 = 0$ m^{-1}, and with $C_{\mathrm{f}} = 4.0$ kg/m^3.

For Simulation 1, the CFL condition (36) is

$$\Delta t \le \left[\frac{4.10 \text{ m/h}}{\Delta z} + \frac{1.55 \text{ m}^2/\text{h}}{(\Delta z)^2} \right]^{-1}.$$

Since $\Delta z = (4 \text{ m})/N$, we get for $N = 90$: $\Delta z = 0.0444$ m ≈ 4 cm and $\Delta t \le 0.00114$ h ≈ 4 s, which is reasonable for this type of spatial detail. A more detailed investigation of this condition is beyond the scope of this paper.

Simulation 1: no dispersion

When $\alpha_1 = 0$ m^{-1} there is no dispersion. The simulation shown in Figure 3(a) shows three steady states and transients between these. The initial steady state is kept for the first 50 h and the other two appear some time after each change in the feed concentration (at $t = 50$ and 250 h, respectively). The third (and final) steady state ($C_{\mathrm{f}} = 4.1$ kg/m^3) has a sludge blanket level slightly higher in the SST and the underflow concentration is higher than in the initial state ($C_{\mathrm{f}} = 4.0$ kg/m^3). During the entire simulation, a discontinuity can be noticed at the feed level.

Simulation 2: dispersion in $|z|<0.4$ m

We now introduce some dispersion around the inlet by setting $\alpha_1 = 0.001$ m^{-1} and $\alpha_2 = 0.0016$ h/m^2, which means that $\alpha_2 Q_{\mathrm{f}} = 0.4$ m is the distance from the inlet where dispersion is present; see Figure 3(b). The (previous) discontinuity at the feed level is now smoothed. In the first part of the simulation where the sludge blanket is quite low, no effect different from Figure 3(a) can be observed. After about 300 h when the sludge blanket rises up into the region of dispersion, the solution is clearly smoothed and the sludge blanket rises up into the clarification zone.

Simulation 3: dispersion in $|z|<0.8$ m

With $\alpha_1 = 0.001$ m^{-1} and $\alpha_2 = 0.0032$ h/m^2, the region of dispersion is now doubled; $\alpha_2 Q_{\mathrm{f}} = 0.8$ m. As Figure 3(c) shows, the initial steady state is smoothed slightly, since the location of the initial sludge blanket is $z = 0.6 < 0.8$ m. As in Figure 3(b), the third steady state contains a sludge blanket in the clarification zone but now at a higher level. Thus, the more dispersion we impose, the higher is the total sludge mass in the SST at steady state. This is clearly seen in Figure 3(d), where the concentration profiles of Simulations 1 and 3 at the end time $t = 800$ h are shown. The effluent concentration is $C_{\mathrm{e}}(t) = 0$ for $0 \le t \le 800$ h for all three simulations. In the final steady state, the underflow concentration C_{u} is therefore uniquely determined by the feed mass flow via the steady-state mass balance $Q_{\mathrm{f}} C_{\mathrm{f}} = Q_{\mathrm{u}} C_{\mathrm{u}}$. Given C_{u}, the steady-state profile is uniquely given by the solution of an ODE; see Bürger *et al.* (2005). Consequently, the steady-state profiles for Simulations 1

and 3 are the same from the bottom up to $z = -0.8$ m, above which there is dispersion in Simulation 3; see Figure 3(d). In Figure 3(e), we can see that as the sludge blanket lies in the dispersion region, which occurs during the first 50 h and after about $t = 240$ h, the concentrations all the way down to the bottom are influenced. This difference in the underflow concentration during transients (less mass leaves the SST during Simulation 3) explains the difference in mass in the final steady states (more mass is contained in the SST at the end of Simulation 3).

Simulation 4: higher Q_f, no dispersion

We apply the same conditions as in Simulation 1, except for the feed and effluent volumetric flows, which are increased by 20 m^3/h to $Q_f = 270$ m^3/h and $Q_e = 190$ m^3/h. Because of the highly located sludge blanket, this small increase in Q_e is sufficient for the SST to become overloaded. Figure 4(a) shows an initial transient with the sludge blanket rising up into the clarification zone. As $C_f = 3.7$ kg/m^3, an almost stationary sludge blanket at about $z = 0.6$ m appears before $t = 250$ h. In the final steady state, the clarification zone is filled with sludge and the flocs are moving upwards slowly since the upward bulk flow (Q_e/A) is only slightly higher than the (downward) settling velocity. Hence, only a small amount of sludge is actually leaving through the effluent at the concentration $C_e(800\text{h}) = 358$ mg/l. Thus, this is an example of a discontinuity arising at the effluent level. The underflow concentration is $C_u(800\text{h}) = 12.99$ kg/m^3 and the steady-state mass

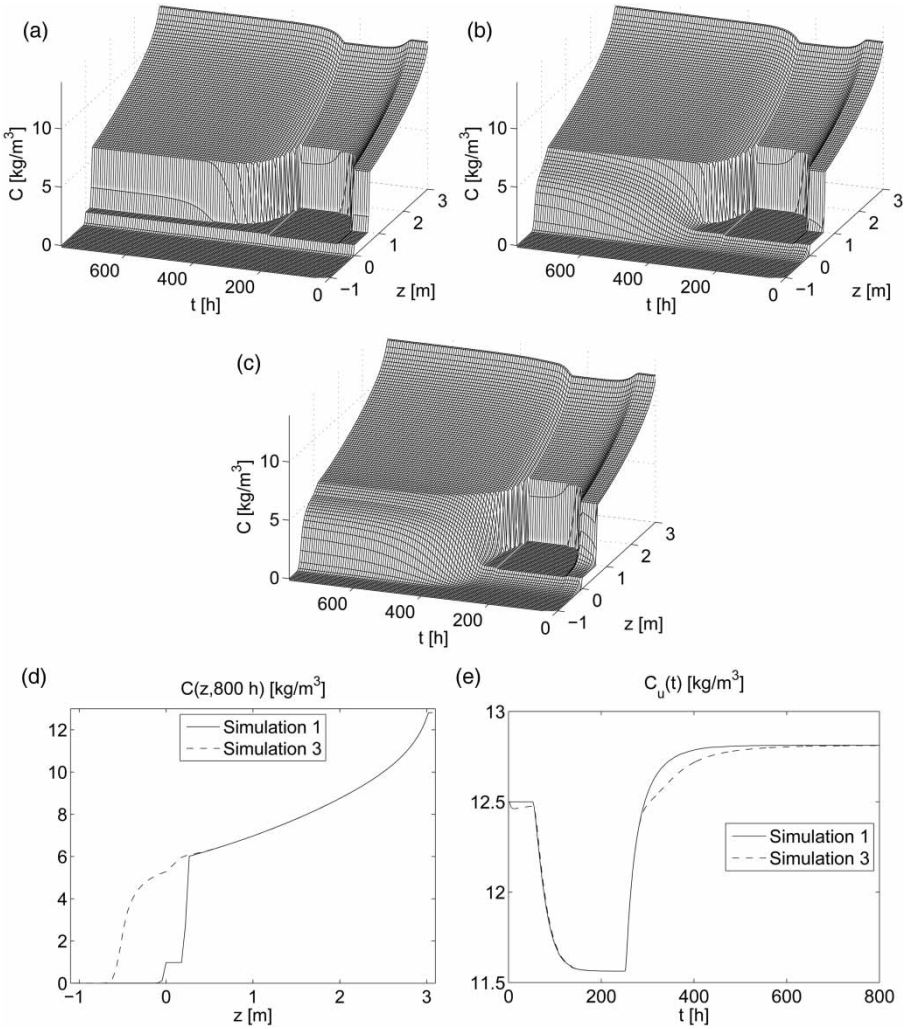

Figure 3 | Three simulations of the same scenario (a)–(c) with different amount of dispersion. Note that compression is present for concentrations above 6 kg/m^3. The last two plots (d)–(e) show details of Simulations 1 and 3.

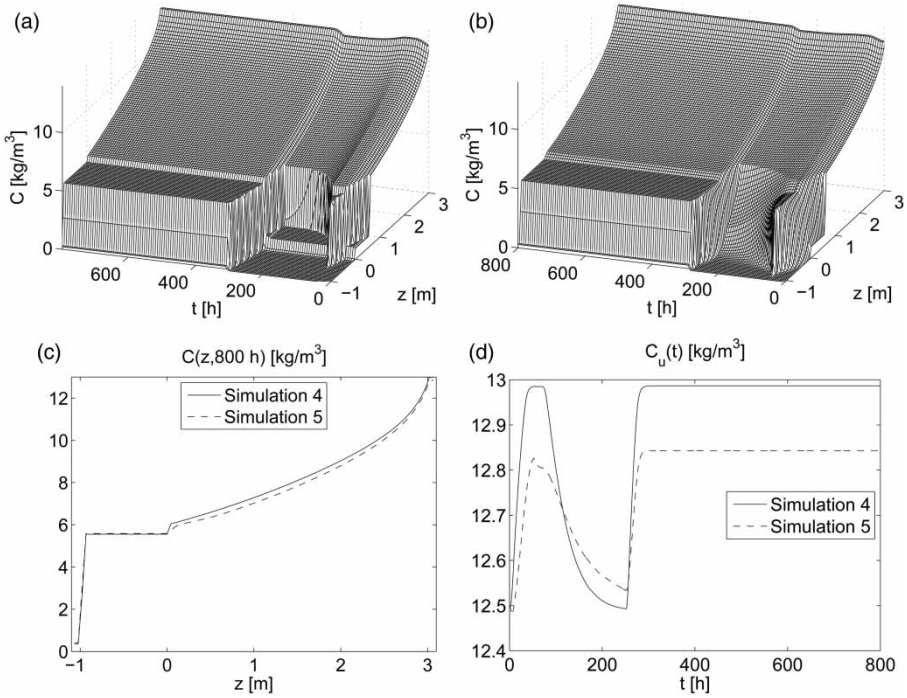

Figure 4 | Simulations 4 and 5 show an overloaded situation without dispersion (a) and with (b). The two concentration profiles along the depth of the SST at the last time point are shown in (c), whereas the underflow concentrations during the simulations are shown in (d).

conservation is satisfied:

$$Q_u C_u + Q_e C_e = 1,038.94 + 68.06 = 1,107.00 = Q_f C_f \quad [\text{kg/h}].$$

Simulation 5: higher Q_f, dispersion in $|z|<0.8$ m

The same conditions as in Simulation 4 are used, but with $\alpha_1 = 0.001\,\text{m}^{-1}$ and $\alpha_2 = 0.8/270\ \text{h/m}^2$, which implies that the region of dispersion is $|z| \le \alpha_2 Q_f = 0.8$ m; see Figure 4(b). In the final steady state, the effluent concentration, $C_e(800\text{h}) = 419$ mg/l, is higher than in Simulation 4. This is an increase of 17% for the same feed load. The dispersion term can thus be used to simulate SSTs that are identical except for different inlet works. To date, we have not seen this feature in the literature. This opens perspectives to include other processes such as flocculation. The underflow concentration $C_u(800\text{h}) = 12.84$ kg/m^3 is lower than in Simulation 4; see Figure 4(c). The steady-state mass conservation is again satisfied:

$$Q_u C_u + Q_e C_e = 1,027.44 + 79.56 = 1,107.00 = Q_f C_f \quad [\text{kg/h}].$$

Note that the mass flow through the effluent is higher, $79.56 - 68.06 = 11.50$ kg/h, with dispersion than without. The different underflow concentrations during Simulations 4 and 5 are shown in Figure 4(d).

DISCUSSION AND CONCLUSIONS

Discussion

Similar, published method-of-lines approaches appear to be equivalent to the present method. However, some differences lead us to believe that some of the previously proposed methods are incorrect, and that others do not offer the flexibility to arbitrarily include or exclude terms in (1). We elucidate this point by some specific examples.

Firstly, it is well known that the common SVT flux (37) yields incorrect results, for example, under wet weather conditions (see references in the 'Introduction'). Thus, a numerical scheme based on (37) may fail to approximate the physically relevant solution. The SVT flux appears in the formulations by Otterpohl & Freund (1992), Watts *et al.* (1996), Chatellier & Audic (2000), David *et al.* (2009a, b), and Abusam & Keesman (2009), and is used in many more published simulations of the ASP, e.g. Cadet *et al.* (2004), Fikar *et al.* (2005), Balku & Berber (2006), Ma *et al.* (2006), Alasino *et al.* (2007), Iacopozzi *et al.* (2007),

Jeppsson *et al.* (2007), Comas *et al.* (2008), Ferrer *et al.* (2008), Guerrero *et al.* (2012), Sin *et al.* (2011), Iratni *et al.* (2012) and Flores-Alsina *et al.* (2012).

Secondly, several of the numerical schemes proposed in the literature rely on the presence of diffusive terms (the second-order terms like those involving our functions d_{comp} and d_{disp}) to smooth out a numerical solution, and do not permit such terms to be set to zero. In fact, David *et al.* (2009a, 2009b) explicitly state that diffusion makes the solution of the initial-boundary value problem easier, and Plósz *et al.* (2007) base their method on an upwind discretization of f_{bk} (in our notation) if global diffusion is present, and replace it by the Godunov flux in the absence of diffusion. Similar limitations are imposed by Chancelier *et al.* (1997), where dispersion is needed near the feed inlet. Furthermore, with the exception of the paper by De Clercq *et al.* (2008) for batch settling, none of the existing papers properly addresses the discretization of a nonlinear and even degenerating compression function d_{comp}. From a physical point of view, a fixed lumped 'dispersion' term also impacts the measured parameters of the settling velocity function, which have to be altered to compensate for the fact that the second-order effects are not modelled explicitly. With respect to the description of compression, we mention that some authors propose to introduce this effect by adding extra terms to the batch flux function f_{bk} (Stricker *et al.* 2007). Although this agrees with the CMM (as discussed by Bürger *et al.* 2011), since the parameters are properly introduced in the constitutive functions only, this procedure seems unsuitable in light of the well-known physical insight that such a constitutive assumption necessarily also involves the gradient of the concentration. This is justified by careful continuum-mechanical derivations including fundamental physical principles; see Aziz *et al.* (2000) and Bürger *et al.* (2005).

Thirdly, numerical implementations that contain heuristically introduced parameters, which cannot be found in the original conservation law of mass (which is equivalent to the model PDE), are bound to be unreliable, e.g. the threshold concentration in the clarification zone by Takács *et al.* (1991), the reduction factor by Plósz *et al.* (2007) and factors in the numerical flux to model compression by Abusam & Keesman (2009).

Fourthly, the conservation of mass should hold everywhere, also across the two outlets of the SST. This implies that in some situations there has to be a concentration discontinuity at the top ($z = -H$) to ensure that the conservation law holds (and similarly at the bottom $z = B$). From a reliable simulator, the concentrations in the top layer inside the SST and in the effluent are outputs, which may be different or equal. It is thus sharply erroneous to assume that they are always equal. Still, the assumption that they are always equal is built into most previously published WWT simulators; see Bürger *et al.* (2012) for references and a detailed explanation of the phenomenon.

Lastly, we mention possible extensions of our model. The activated sludge consists of flocs with a wide size distribution (polydisperse suspension). One may distinguish between several floc size classes, which is the basic idea of the model by McCorquodale *et al.* (2004); see also Griborio (2004). This may improve the accuracy and the predictive power of the method, especially in the dilute regime. However, for the proper combination with the compression effect (via the gradient of concentrations of species), a suitable extension of the present model to handle several particle classes could be based on the work by Stamatakis & Tien (1992) or Berres *et al.* (2003). This leads to a coupled system of scalar PDEs (each one akin to (1)) for the concentrations of all species. A further step would consist in combining such a model for the spatio-temporal evolution of solid flocs distribution with a population balance approach (Parker *et al.* 1970, 1971; Ramkrishna 2000) for including floc aggregation and breakage.

Conclusions

The derivation and implementation of a numerical method for 1D simulation of SSTs is presented. The simulation method has the following features.

- It is derived from the conservation law of mass supported by PDE theory and adherent numerical analysis. No heuristic parameters are introduced in the numerical method and no assumptions on the solution are made, such as the concentration is continuous across the outlets. In Simulation 4, we have demonstrated that there may be a concentration discontinuity at the effluent level as part of the solution.
- It is reliable in the sense that it produces correct numerical approximations of the exact solution of the model PDE. This means that it is also robust, since it can handle all possible situations and choices of number of layers. Necessary ingredients are the extra layers outside the SST, the time-step limitation (CFL condition) and careful discretizations of the convection and compression terms.
- According to CMM, all model parameters are introduced only in the physical constitutive relations, which comprise hindered sedimentation, compression of particles at high concentrations and dispersion that depends on depth and volumetric feed flow.

- It is more general than published 1D simulation methods, since reliable simulations are obtained irrespective of whether the modelling phenomena of compression and dispersion are turned on or off, separately. Any function for the hindered settling velocity can be used, e.g. the double-exponential function by Takács *et al.* (1991) to account for small particles that are usually found in the effluent suspended solids. This allows for a stepwise calibration and validation of different parts of the simulator.
- Simulations indicate that, although dispersion is localized around the inlet, it influences all concentrations in the SST during transient situations and in overloaded steady states. In other steady states ($C_e = 0$), dispersion around the inlet only influences the concentrations locally, so that the underflow concentration is not influenced. However, the total sludge mass in the SST is increased.
- The physically correct Godunov numerical flux is computed in a fast and simple way (Algorithm 1). This flux can be viewed as a direct extension of the well-known SVT flux.
- The Takács simulation model, which has served the community for over 20 years and still is in use in many commercial simulators, can now fairly easily be upgraded to the presented reliable simulation model, which includes additional effects that can be customarily chosen.

ACKNOWLEDGEMENTS

RB, SD and SF acknowledge support by Conicyt (Chile) through Fondecyt project 1090456. RB is also supported by Red Doctoral REDOC.CTA, project UCO1202 at Universidad de Concepción; by Conicyt through BASAL project CMM, Universidad de Chile and Centro de Investigación en Ingeniera Matemática (CI^{2}MA), Universidad de Concepción; and project Anillo ACT1118 (ANANUM). SF has also been supported by MECESUP (Programa de Mejoramiento de la Calidad y Equidad de la Educación; Chile), project UCO0713 and by the Crafoord Foundation, Sweden (grant 20110535). SD acknowledges partial support by the Foundation for Engineering Scientific Research to the Memory of J. Gust. Richert, Sweco AB, Sweden. IN and ET thank the Flemish Fund for Scientific Research (Project G.A051.10).

REFERENCES

Abusam, A. & Keesman, K. J. 2009 Dynamic modeling of sludge compaction and consolidation processes in wastewater secondary settling tanks. *Water Environ. Res.* **81** (1), 51–56.

Alasino, N., Mussati, M. C. & Scenna, N. 2007 Wastewater treatment plant synthesis and design. *Ind. Eng. Chem. Res.* **46** (23), 7497–7512.

Anderson, H. M. & Edwards, R. V. 1981 A finite difference scheme for the simulation of continuous sedimentation. *AIChE Symp. Ser.* **77** (209), 227–238.

Attir, U. & Denn, M. M. 1978 Dynamics and control of the activated sludge wastewater process. *AIChE J.* **24**, 693–698.

Aziz, A. A. A., de Kretser, R. G., Dixon, D. R. & Scales, P. J. 2000 The characterisation of slurry dewatering. *Water Sci. Technol.* **41** (8), 9–16.

Balku, S. & Berber, R. 2006 Dynamics of an activated sludge process with nitrification and denitrification: start-up simulation and optimization using evolutionary algorithm. *Comput. Chem. Eng.* **30** (3), 490–499.

Berres, S., Bürger, R., Karlsen, K. H. & Tory, E. M. 2003 Strongly degenerate parabolic-hyperbolic systems modeling polydisperse sedimentation with compression. *SIAM J. Appl. Math.* **64**, 41–80.

Bürger, R. & Karlsen, K. H. 2001 On some upwind schemes for the phenomenological sedimentation-consolidation model. *J. Eng. Math.* **41**, 145–166.

Bürger, R., Karlsen, K. H. & Towers, J. D. 2005 A model of continuous sedimentation of flocculated suspensions in clarifier-thickener units. *SIAM J. Appl. Math.* **65**, 882–940.

Bürger, R., Diehl, S. & Nopens, I. 2011 A consistent modelling methodology for secondary settling tanks in wastewater treatment. *Water Res.* **45**, 2247–2260.

Bürger, R., Diehl, S., Farås, S. & Nopens, I. 2012 On reliable and unreliable numerical methods for the simulation of secondary settling tanks in wastewater treatment. *Comput. Chem. Eng.* **41**, 93–105.

Cacossa, K. F. & Vaccari, D. A. 1994 Calibration of a compressive gravity thickening model from a single batch settling curve. *Water Sci. Technol.* **30**, 107–116.

Cadet, C., Beteau, J. F. & Carlos-Hernandez, S. 2004 Multicriteria control strategy for cost/quality compromise in wastewater treatment plants. *Control Eng. Pract.* **12** (3), 335–347.

Chancelier, J. P., Cohen de Lara, M., Joannis, C. & Pacard, F. 1997 New insights in dynamic modeling of a secondary settler – II. Dynamical analysis. *Water Res.* **31**, 1857–1866.

Chatellier, P. & Audic, J. M. 2000 A new model for wastewater treatment plant clarifier simulation. *Water Res.* **34**, 690–693.

Comas, J., Rodríguez-Roda, I., Gernaey, K. V., Rosen, C., Jeppsson, U. & Poch, M. 2008 Risk assessment modelling of microbiology-related solids separation problems in activated sludge systems. *Environ. Model. Softw.* **23** (10–11), 1250–1261.

David, R., Saucez, P., Vasel, J.-L. & Vande Wouwer, A. 2009a Modeling and numerical simulation of secondary settlers: a method of lines strategy. *Water Res.* **43** (2), 319–330.

David, R., Vasel, J.-L. & Vande Wouwer, A. 2009b Settler dynamic modeling and MATLAB simulation of the activated sludge process. *Chem. Eng. J.* **146**, 174–183.

De Clercq, J., Devisscher, M., Boonen, I., Vanrolleghem, P. A. & Defrancq, J. 2003 A new one-dimensional clarifier model – verification using full-scale experimental data. *Water Sci. Technol.* **47** (12), 105–112.

De Clercq, J., Jacobs, F., Kinnear, D. J., Nopens, I., Dierckx, R. A., Defrancq, J. & Vanrolleghem, P. A. 2005 Detailed spatio-temporal solids concentration profiling during batch settling of activated sludge using a radiotracer. *Water Res.* **39**, 2125–2135.

De Clercq, J., Nopens, I., Defrancq, J. & Vanrolleghem, P. A. 2008 Extending and calibrating a mechanistic hindered and compression settling model for activated sludge using in-depth batch experiments. *Water Res.* **42**, 781–791.

Diehl, S. 2000 On boundary conditions and solutions for ideal clarifier-thickener units. *Chem. Eng. J.* **80**, 119–133.

Diehl, S. & Jeppsson, U. 1998 A model of the settler coupled to the biological reactor. *Water Res.* **32** (2), 331–342.

Dupont, R. & Henze, M. 1992 Modelling of the secondary clarifier combined with the Activated Sludge Model No. 1. *Water Sci. Technol.* **25** (6), 285–300.

Ekama, G. A., Barnard, J. L., Günthert, F. W., Krebs, P., McCorquodale, J. A., Parker, D. S. & Wahlberg, E. J. 1997 *Secondary Settling Tanks: Theory, Modelling, Design and Operation*. IAWQ scientific and technical report no. 6. International Association on Water Quality, London, UK.

Engquist, B. & Osher, S. 1981 One-sided difference approximations for nonlinear conservation laws. *Math. Comp.* **36**, 321–351.

Ferrer, J., Seco, A. & Serralta, J. 2008 DESASS: a software tool for designing, simulating and optimising WWTPs. *Environ. Model. Softw.* **23** (1), 19–27.

Fikar, M., Chachuat, B. & Latifi, M. A. 2005 Optimal operation of alternating activated sludge processes. *Control Eng. Pract.* **13** (7), 853–861.

Flores-Alsina, X., Gernaey, K. V. & Jeppsson, U. 2012 Benchmarking biological nutrient removal in wastewater treatment plants: influence of mathematical model assumptions. *Water Sci. Technol.* **65** (8), 1496–1505.

Giokas, D. L., Kim, Y., Paraskevas, P. A., Paleologos, E. K. & Lekkas, T. D. 2002 A simple empirical model for activated sludge thickening in secondary clarifiers. *Water Res.* **36**, 3245–3252.

Godunov, S. K. 1959 Finite difference methods for numerical computation of discontinuous solutions of equations of fluid dynamics. *Mat. Sb.* **47**, 271–295 (in Russian).

Griborio, A. 2004 *Secondary Clarifier Modeling: A Multi-Process Approach*, PhD Thesis, University of New Orleans, New Orleans, LA, USA.

Guerrero, J., Guisasola, A., Vilanova, R. & Baeza, J. A. 2012 Improving the performance of a WWTP control system by model-based setpoint optimisation. *Environ. Model. Softw.* **26** (4), 492–497.

Härtel, L. & Pöpel, H. J. 1992 A dynamic secondary clarifier model including processes of sludge thickening. *Water Sci. Technol.* **25** (6), 267–284.

Iacopozzi, I., Innocenti, V., Marsili-Libelli, S. & Giusti, E. 2007 A modified activated sludge model no. 3 (ASM3) with two-step nitrification-denitrification. *Environ. Model. Softw.* **22** (6), 847–861.

Iratni, A., Katebi, R. & Mostefai, M. 2012 On-line robust nonlinear state estimators for nonlinear bioprocess systems. *Commun. Nonlinear Sci. Numer. Simulat.* **17**, 1739–1752.

Jeppsson, U. & Diehl, S. 1996a An evaluation of a dynamic model of the secondary clarifier. *Water Sci. Technol.* **34** (5–6), 19–26.

Jeppsson, U. & Diehl, S. 1996b On the modelling of the dynamic propagation of biological components in the secondary clarifier. *Water Sci. Technol.* **34** (5–6), 85–92.

Jeppsson, U., Pons, M.-N., Nopens, I., Alex, J., Copp, J., Gernaey, K. V., Rosen, C., Steyer, J.-P. & Vanrolleghem, P. A. 2007 Benchmark simulation model No 2 – general protocol and exploratory case studies. *Water Sci. Technol.* **56** (8), 67–78.

Koehne, M., Hoen, K. & Schuhen, M. 1995 Modelling and simulation of final clarifiers in wastewater treatment plants. *Math. Comput. Simul.* **39** (5–6), 609–616.

Kynch, G. J. 1952 A theory of sedimentation. *Trans. Farad. Soc.* **48**, 166–176.

Lee, T. T., Wang, F. Y. & Newell, R. B. 2006 Advances in distributed parameter approach to the dynamics and control of activated sludge processes for wastewater treatment. *Water Res.* **40** (5), 853–869.

Lev, O., Rubin, E. & Sheintuch, M. 1986 Steady state analysis of a continuous clarifier-thickener system. *AIChE J.* **32**, 1516–1525.

Le Veque, R. J. 1992 *Numerical Methods for Conservation Laws* 2nd edn, Birkhäuser Verlag, Basel, Switzerland.

Ma, Y., Peng, Y. & Wang, S. 2006 New automatic control strategies for sludge recycling and wastage for the optimum operation of predenitrification processes. *J. Chem. Technol. Biotechnol.* **81** (1), 41–47.

Martin, A. D. 2004 Optimisation of clarifier-thickeners processing stable suspensions for turn-up/turn-down. *Water Res.* **38**, 1568–1578.

Mazzolani, G., Pirozzi, F. & d'Antonoi, G. 1998 A generalized settling approach in the numerical model of sedimentation tanks. *Water Sci. Technol.* **38** (3), 95–102.

McCorquodale, J. A., La Motta, E., Griborio, A., Georgiou, I. & Homes, J. 2004 *Development of Software for Modeling Activated Sludge Clarifier System*. Technology Transfer Report Submitted to US EPA, Schielder Urban Environmental System Center, University of New Orleans, New Orleans, LA, USA.

Otterpohl, R. & Freund, M. 1992 Dynamic models for clarifiers of activated sludge plants with dry and wet weather flows. *Water Sci. Technol.* **26** (5–6), 1391–1400.

Parker, D. S., Kaufman, W. J. & Jenkins, D. 1970 *Characteristics of Biological Floc in Turbulent Regimes*. SERL Report 70–5, University of California, Berkeley, CA, USA.

Parker, D. S., Kaufman, W. J. & Jenkins, D. 1971 Physical conditioning of activated sludge flocs. *J. Water Pollut. Control Fed.* **43** (9), 1817–1834.

Plósz, B. G., Weiss, M., Printemps, C., Essemiani, K. & Meinhold, J. 2007 One-dimensional modelling of the secondary

clarifier – factors affecting simulation in the clarification zone and the assessment of the thickening flow dependence. *Water Res.* **41**, 3359–3371.

Plósz, B. G., Nopens, I., De Clercq, J., Benedetti, L. & Vanrolleghem, P. A. 2011 Shall we upgrade one-dimensional secondary settler models used in WWTP simulators? – an assessment of model structure uncertainty and its propagation. *Water Sci. Technol.* **63** (8), 1726–1738.

Queinnec, I. & Dochain, D. 2001 Modelling and simulation of the steady-state of secondary settlers in wastewater treatment plants. *Water Sci. Technol.* **43** (7), 39–46.

Ramkrishna, D. 2000 *Population Balances: Theory and Applications to Particulate Systems in Engineering*. Academic Press, London, UK.

Sin, G., Gernaey, K. V., Neumann, M. B., Van Loosdrecht, M. C. M. & Gujer, W. 2011 Global sensitivity analysis in wastewater treatment plant model applications: prioritizing sources of uncertainty. *Water Res.* **45** (2), 639–651.

Stamatakis, K. & Tien, C. 1992 Batch sedimentation calculations – the effect of compressible sediment. *Powder Technol.* **72**, 227–240.

Stenstrom, M. K. 1976 *A Dynamic Model and Computer Compatible Control Strategies for Wastewater Treatment Plants*. PhD Dissertation, Clemson University, Clemson, SC, USA.

Stricker, A.-E., Takacs, I. & Marquot, A. 2007 Hindered and compression settling: parameter measurement and modelling. *Water Sci. Technol.* **56** (12), 101–110.

Takács, I., Patry, G. G. & Nolasco, D. 1991 A dynamic model of the clarification-thickening process. *Water Res.* **25**, 1263–1271.

Vaccari, D. A. & Uchrin, C. G. 1989 Modeling and simulation of compressive gravity thickening of activated sludge. *J. Environ. Sci. Health* **A24** (6), 645–674.

Verdickt, L., Smets, I. & Van Impe, J. 2005 Sensitivity analysis of a one-dimensional convection-diffusion model for secondary settling tanks. *Chem. Eng. Commun.* **192**, 1567–1585.

Vesilind, P. A. 1968 Design of prototype thickeners from batch settling tests. *Water Sewage Works* **115**, 302–307.

Vitasovic, Z. 1989 Continuous settler operation; a dynamic model. In: *Dynamic Modeling and Expert Systems in Wastewater Engineering* (G. G. Patry & D. Chapman, eds). Lewis Publishers, Chelsea, MI, USA, pp. 59–81.

Watts, R. W., Svoronos, S. A. & Koopman, B. 1996 One-dimensional modeling of secondary clarifiers using a concentration and feed velocity-dependent dispersion coefficient. *Water Res.* **30**, 2112–2124.

Wett, B. 2002 A straight interpretation of the solids flux theory for a three-layer sedimentation model. *Water Res.* **36**, 2949–2958.

First received 24 October 2012; accepted in revised form 4 March 2013